Article

Not peer-reviewed version

Tracking Control of Uncertain Neural-Network Systems With Preisach Hysteresis Inputs: A New Iteration-Based Adaptive Inversion Approach

Guanyu Lai , Gongqing Deng , Weijun Yang * , Xiaodong Wang , Xiaohang Su

Posted Date: 27 July 2023

doi: 10.20944/preprints202307.1915.v1

Keywords: Adaptive control; neural networks; stability analysis; piezoactuators; noncanonical nonlinear systems

Article

Tracking Control of Uncertain Neural-Network Systems With Preisach Hysteresis Inputs: A New Iteration-Based Adaptive Inversion Approach

Guanyu Lai [1], Gongqing Deng [1], Weijun Yang [2,*], Xiaodong Wang [2] and Xiaohang Su [3]

[1] School of Automation, Guangdong University of Technology, Guangzhou 510006, China; lgy124@gdut.edu.cn(G.L.); 3120001076@mail2.gdut.edu.cn(G.D.);
[2] School of Mechanical and Electrical Engineering, Guangzhou City Polytechnic, Guangzhou 510405, China;
[3] School of Computer Science & Engineering, South China University of Technology, Guangzhou 510006, China; suxh@scut.edu.cn
* Correspondence: ywj@gcp.edu.cn (W.Y.)

Abstract: To describe the hysteresis nonlinearities in smart actuators, numerous models have been presented in the literature, among which the Preisach operator would be the most effective one due to its capability in capturing multi-loop or sophisticated hysteresis curves. When such an operator is coupled with uncertain nonlinear dynamics, especially in noncanonical form, it is a challenging problem to develop techniques to cancel out the hysteresis effects, and at the same time achieve asymptotic tracking performance. To resolve this problem, in this paper, we investigate the problem of iterative inverse-based adaptive control for an uncertain noncanonical nonlinear systems with unknown input Preiasch hysteresis, and a new adaptive version of the closest match algorithm is proposed to compensate for the Preisach hysteresis. With our scheme, the stability and convergence of the closed-loop system can be established. The effectiveness of the proposed control scheme is illustrated by simulation and experiment results.

Keywords: adaptive control; neural networks; stability analysis; piezoactuators; noncanonical nonlinear systems

1. Introduction

Hysteresis widely occurs in the smart material-based actuators [1–3], such as electromagnetic actuators [4] and piezoelectric actuators [5]. Experiments show the system with hysteresis would perform poor tracking performance when the feedback control without explicitly considering hysteresis [6]. In order to compensate for the hysteresis nonlinearity in control design, a mathematical operator that can describe the characteristics of the hysteresis nonlinearity is needed. In the literature, the commonly used hysteresis models include the Preisach operator [7,8], the Duhem operator [9], the PrandtI-Ishlinskii (PI) operator [10], etc, among which the Preisach operator would be the most effective one due to its general and well-established mathematical structure and the ability in capturing multi-loop hysteresis curves and asymmetric hysteresis curves, where the hysteresis nonlinearity is modeled by a superposition of infinity weighted elementary relays. Then, the question naturally arises that how to compensate for the Preisach-type hysteresis nonlinearity.

It is well known that the traditional robust control methods are effective to accommodate the nonlinearities in the controlled system [11–13]. However, such control approaches cannot compensate for the hysteresis nonlinearity well and would lead to a significant degradation in the tracking performance of the system when the effects of hysteresis nonlinearity are considerable. Therefore, it becomes needed to employ some advanced methods for compensating the hysteresis nonlinearity. ln this regard, one of the fundamental approaches in effectively addressing hysteresis nonlinearity is inverse compensation[14–18], which aims to reduce or eliminate the hysteresis effects by constructing an approximate or right inverse hysteresis model. However, different from some certain hysteresis models, such as the PI operator (as a special case of the Preisach operator) and the Duhem operator, it

 doi:10.20944/preprints202307.1915.v1

is challenging to compute the analytical inverse of the Preisach operator. This difficulty arises due to the implicit involvement of the input signal within the operator [19].

To overcome the above challenge, Tan, Venkataraman, and Krishnaprasad propose the closest match algorithm [20], which is a classical iterative approximation algorithm for the Preisach inverse. In such an algorithm, the number of iterations does not exceed the discretization degree of the input, and the state of the thermostat relay operator (1) changes only once for each solution, which greatly saves the computation time [20,21]. By requiring the piecewise monotonicity and Lipschitz continuity of the Preisach operator and letting the density function be nonnegative and constant, the approximate inverse model based on the closest match algorithm is proposed in [22], for calculating the inverse of the Prerisach operator iteratively, and the convergence of the algorithm is proved. When the density function of the Preisach operator is unknown or not available for measurement, the previously mentioned open-loop inverse control is not available. In this case, the feedback information obtained from the hysteresis output can be utilized to estimate the density function of the Preisach operator by developing an iterative algorithm with an adaptive estimator, and ultimately reducing the inversion error. The above-mentioned iterative adaptive inverse control framework has been established in [21,23]. For an individual Preisach operator, the compensation scheme has been studied in great depth. However, these results only consider the hysteresis nonlinearity while neglecting the influence of the plant. When the Preisach operator couples with some system dynamics (for example, smart material-based actuators can be modeled as a Preisach operator precedes linear dynamics [24] or when the hysteretic actuator modeled by Preisach operator drives linear or nonlinear dynamics [21,25]), it is an unsolved and challenging problem to develop a new adaptive version of the closest match algorithm for compensating the Preisach hysteresis with complete convergence proof and stability analysis, especially when the dynamics of system are described as the noncanonical nonlinear system with parametric uncertainties [26].

The work of this paper is to develop an adaptive inverse control scheme for uncertain noncanonical nonlinear system with unknown input Preisach hysteresis. In scenarios where the Preisach operator precedes the dynamics of an uncertain noncanonical nonlinear systems, the hysteresis parameters, the hysteresis output, and the system parameters are all unknown and also the relative degree structure is implicit. In this situation, we propose an iterative adaptive inverse algorithm for the Preisach operator to effectively compensate for the hysteresis nonlinearity, where the adaptive estimator in the iterative algorithm is updated online. In summary, the work of this study has the following contributions:

1) A Lyapunov-based adaptive control scheme is proposed for uncertain noncanonical nonlinear systems with Preisach hysteresis inputs, with which all closed-loop signals can be ensured bounded, and the tracking error is steered into zero.

2) For our scheme, an adaptive version of the closest-matching is newly proposed to solve the inversion problem of the Preisach operator with unknown density function, and based on the piecewise-monotonicity and Lipschitz-continuity properties of the adaptive Preisach operator, the convergence of the iteration algorithm for inverting the Preisach operator is successfully established.

3) Besides theoretical analysis, the obtained results are also verified by simulation and experiment tests.

The rest of the paper is organized as follows. In Section 2, we introduce the Preisach operator and formulate the control problem. In Section 3, by utilizing the feedback linearization technique, we derive a certain condition to define the relative degree of neural-network approximation system in noncanonical form. In Section 4, we propose an adaptive tracking control scheme containing an iterative adaptive inverse algorithm for an uncertain neural-network approximation system with unknown input Preisach hysteresis, which is the main work of this paper. In Section 5, we give a simulation example with the corresponding results, which validate that the control scheme is effective. Finally, We give the conclusion in Section 6.

Preprints (www.preprints.org) | NOT PEER-REVIEWED | Posted: 27 July 2023 doi:10.20944/preprints202307.1915.v1

2. Background And System Modelling

This section provides a concise review of the Preisach operator and applies it to effectively capture the complex hysteresis nonlinearity discussed in this paper, and the control problem is formulated later.

2.1. The Hysteresis Model

The Preisach operator stands out among various hysteresis models due to its capability to accurately represent complex hysteresis curves, including multi-loop and asymmetric hysteresis curves, and it is constructed by the weighted superposition of infinity basic relay operators. Typically, the thermostat relay operators [21] are chosen as the fundamental components for constructing the Preisach operator as shown in Figure 1.

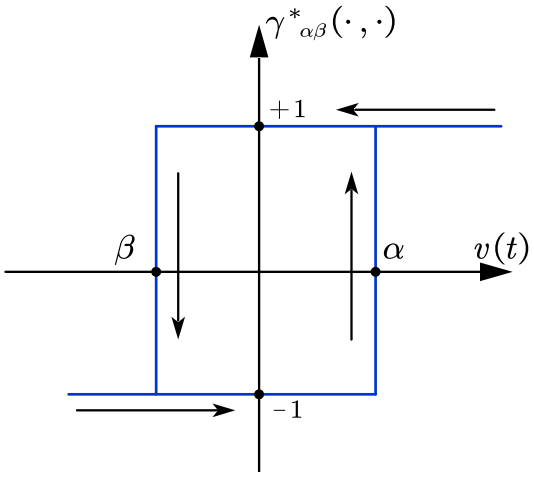

Figure 1. A thermostat relay operator $\gamma^*_{\alpha\beta}(\cdot,\cdot)$.

Thermostat relay operator: We first consider the Preisach plane as

$$T_0 = \{(\beta,\alpha) \in |\beta \geq \beta_0, \alpha \leq \alpha_0, \alpha \geq \beta\},$$

which is a right triangle area and is consisted of a vertex coordinate (β_0,α_0) and a part of line $\alpha = \beta$. For a visual representation, we present the geometric interpretation of the Preisach plane T_0 in Figure 2. For any given point (β,α) on the Preisach plane T_0, there is a corresponding thermostat relay operator

$$\begin{aligned}&\gamma^*_{\alpha\beta}\left(v(t),\tau_0(\beta,\alpha)\right)\\ &\quad=\begin{cases}+1, & \text{if} \quad v(t)>\alpha\\ -1, & \text{if} \quad v(t)<\beta\\ \text{remain unchanged}, & \text{if} \quad v(t)\in[\beta,\alpha],\end{cases}\end{aligned} \tag{1}$$

where $v(t) \in [0,t_m]$ is the input of the thermostat relay operator with continuity and piecewise monotonicity and $\tau_0(\beta,\alpha)$ represents the initial value of the thermostat relay operator $\gamma^*_{\alpha\beta}(v(0),\cdot)$. For example, $\tau_0(\beta,\alpha) = 1$ while $\forall(\beta,\alpha) \in T_0$ and $v(0) > \alpha_0$.

Preisach operator: The Preisach operator is constructed by the weighted superposition of infinity thermostat relay operators on the Preisach plane T_0, which is presented as follows

$$\begin{aligned}u(t) &= \mathcal{H}(v(t),\tau_0(\beta,\alpha))\\ &= \iint_{T_0}\mu(\beta,\alpha)\gamma^*_{\alpha\beta}\left(v(t),\tau_0(\beta,\alpha)\right)d\beta d\alpha,\end{aligned} \tag{2}$$

Preprints (www.preprints.org) | NOT PEER-REVIEWED | Posted: 27 July 2023 doi:10.20944/preprints202307.1915.v1

where the weighting function $\mu(\beta,\alpha)$ also referred to the density function, and according to the definition of the Preisach operator, all points $(\beta,\alpha) \in T_0$ have the corresponding density function $\mu(\beta,\alpha) \neq 0$ and when $(\beta,\alpha) \notin T_0$, the density function $\mu(\beta,\alpha) = 0$ as shown in Figure 2.

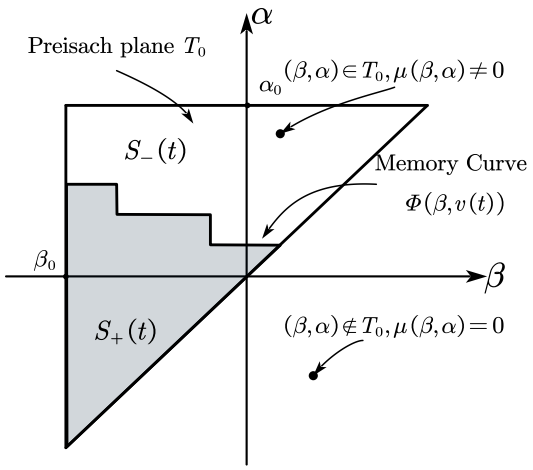

Figure 2. The Preisach plane T_0 and memory curve.

Memory curve: The memory effects of the Preisach operator can be captured by the memory curve in the Preisach plane T_0 (as illustrated in [21]). When the Preisach input increases monotonically, the output of the thermostat relay operator above the α threshold switches to $+1$ and forms an upward-shifting curve. Similarly, when the Preisach input decreases monotonically, the output of the thermostat relay operator below the β threshold switches to -1 and forms a leftward-shifting curve. Then, in the Preisach plane T_0, a piecewise monotone input signal $v(t)$ can create the memory curve $\Phi(\beta, v(t))$ as shown in Figure 2, where the memory curve divides the plane T_0 into two parts:

$$\begin{aligned} S_+(t) &= \left\{(\beta,\alpha) \in T_0 \mid \gamma^*_{\alpha\beta}(v(t),\cdot) = +1\right\}, \\ S_-(t) &= \left\{(\beta,\alpha) \in T_0 \mid \gamma^*_{\alpha\beta}(v(t),\cdot) = -1\right\}, \end{aligned} \tag{3}$$

and we can rewrite the integral (2) as

$$\begin{aligned} u(t) &= \mathcal{H}(v(t), \tau_0(\beta,\alpha)) \\ &= \iint_{S_+(t)} \mu(\beta,\alpha)d\beta d\alpha - \iint_{S_-(t)} \mu(\beta,\alpha)d\beta d\alpha \\ &= 2\iint_{S_+(t)} \mu(\beta,\alpha)d\beta d\alpha - \iint_{T_0} \mu(\beta,\alpha)d\beta d\alpha, \end{aligned} \tag{4}$$

which is an essential form to analyze the output range of the Preisach operator and to prove the piecewise monotonicity of the adaptive Preisach operator.

Following the description of the Preisach operator, we proceed to introduce the considered plant model and formulate the adaptive control problem.

2.2. System Modeling

Consider the following uncertain noncanonical nonlinear system with unknown input Preiasch hysteresis:

$$\begin{aligned} \dot{x}(t) &= \mathcal{N}(x(t)) + Bu(t), \\ y(t) &= Cx(t), \quad u(t) = \mathcal{H}(v(t), \tau_0(\beta,\alpha)), \end{aligned} \tag{5}$$

Preprints (www.preprints.org) | NOT PEER-REVIEWED | Posted: 27 July 2023 doi:10.20944/preprints202307.1915.v1

where the $\mathcal{N}(x(t)) \in \mathbb{R}^n$ represent the unknown unparametrizable system nonlinearities, $x(t) \in \mathbb{R}^n$ denotes the system state vector, $y(t) \in \mathbb{R}$ denotes the system output, $B \in \mathbb{R}^n, C \in \mathbb{R}^{1\times n}$ are the unknown system parameters, the control input $v(t) \in \mathbb{R}^n$ contains in the Preisach operator implicitly and $u(t)$ is the Preisach output, which applies to the system directly. Since the Preisach hysteresis parameters $\mu(\beta, \alpha)$ are unknown, the output of the Preisach operator $u(t)$ is not available for measurement, which poses a difficulty in compensating for hysteresis nonlinearity.

An approximation system: In our research, the system nonlinearities $\mathcal{N}(\cdot)$ in (5) cannot be fully parameterized and are considered to be unknown, which poses a challenge in designing the control scheme for the original system (5) due to the lack of explicit characterization of these nonlinearities. To overcome such a challenge, we construct a parametrizable neural-network approximation system, which serves as an equivalent representation of the original system (5) over any desired compact set $\Psi \in \mathbb{R}^n$ [26], which has the form as follows

$$\begin{aligned} \dot{x}(t) &= Ax(t) + \mathcal{W}^* S(x(t)) + Bu(t), \\ y(t) &= Cx(t), \quad u(t) = \mathcal{H}(v(t), \tau_0(\beta, \alpha)), \end{aligned} \tag{6}$$

where $A \in \mathbb{R}^{n\times n}$ is a stable martrix, $\mathcal{W}^* \in \mathbb{R}^{n\times l}$, $S(x(t)) \in \mathbb{R}^l$ is an unknown connection weigth martrix and a known activation functions vector, respectively.

Remark 1. *The nonlinear term $\mathcal{W}^* S(\cdot)$ in (6) is considered as the parameterizable uncertainties, which is capable to approximate unparametrizable uncertainties with arbitrary accuracy on a desired compact set. Hence, the proposed control scheme for the approximation system (6) in this paper is valid for the general noncanonical nonlinear system (5) with unparametrizable nonlinearities. By leveraging the neural-network approximation system as an equivalent representation, our control scheme provides a practical and viable solution for achieving desired control performance with unknown input Preisach hysteresis.*

Considering the constructed approximation system (6), our control objective is to design a control input signal $v(t)$ by cooperating the Lyapunov method with the iterative algorithm to ensure that the signals within the closed-loop system are bounded, and to achieve the asymptotic tracking performance.

3. Relative Degree Conditions and Stability of Zero Dynamics Subsystem

In this paper, our main focus is on dealing with the control problem for noncanonical nonlinear systems with input hysteresis by adaptive control techniques, specifically in the relative-degree-one case. It should be pointed out that the relative degree greater than one case remains an open area for future research and will be considered in our future work. This noncanonical neural network system can be considered as a general nonlinear system so that the feedback linearization theory can be used to define its relative degree and later we will give the certain condition of the relative-degree-one case.

Relative Degree Conditions: By combining the definition of relative degree [27] with the noncanonical nonlinear system (6), we establish the following necessary condition for the cases where the system has a relative degree of one.

Lemma 1. *The approximation system (6) preceded by the Preisach operator has relative degree $\varrho = 1$ if and only if*

$$CB \neq 0. \tag{7}$$

The approximation system (6) can be equivalently transformed into the general nonlinear system $\dot{x}(t) = f_0(t) + g_0(t)u(t), y(t) = Cx(t)$, and from the feedback linearization conclusions, Lemma 1 can be proved straightforwardly.

Preprints (www.preprints.org) | NOT PEER-REVIEWED | Posted: 27 July 2023 doi:10.20944/preprints202307.1915.v1

Lemma 2. *Suppose the approximation system (6) has relative degree ϱ on the compact set Ψ. To facilitate analysis and control design, we employ a diffeomorphism $\Omega(x) = [T_c^T(x), T_z^T(x)]^T \in \mathbb{R}^n$ where*

$$\begin{aligned} T_c(x) = \xi(t) &= [\xi_1(t), \xi_2(t), \cdots, \xi_\varrho(t)]^T \\ &= [h_0(x), L_{f_0}h_0(x), \cdots, L_{f_0}^{\varrho-1}h_0(x)] \in \mathbb{R}^\varrho, \\ T_z(t) &= \eta(t) \in \mathbb{R}^{n-\varrho}, \end{aligned}$$

which can transform the system into two subsystems [28]. The first subsystem, known as the tracking dynamics subsystem, is dedicated to achieving accurate tracking of a desired reference signal, and it is defined as follows

$$\begin{aligned} \dot{\xi}_k(t) &= \xi_{k+1}(t), k = 1, 2, \cdots, \varrho - 1, \\ \dot{\xi}_\varrho(t) &= L_f^\varrho h(x) + L_g L_f^{g-1} h(x) u(t), \end{aligned} \tag{8}$$

The second subsystem, referred to as the zero dynamics subsystem, is of great importance to ensure the convergence and stability of the system's internal dynamics. It has the form as follows

$$\dot{\eta}(t) = \Xi(\xi(t), \eta(t)). \tag{9}$$

Stability of the zero dynamics system: By utilizing the feedback linearization technique, the approximate system (6) can be divided into two subsystems (as illustrated in Lemma 2). The zero dynamic subsystems among them does not contain control inputs. Therefore, the stability of the zero dynamic subsystem needs to be guaranteed to ensure that the control scheme developed for the noncanonical nonlinear system with input hysteresis in this paper is available. The following Assumption will satisfy our requirement.

Assumption 1. *The partial derivatives of the zero dynamics subsystem with respect to $\xi(t)$ (9) are bounded, and the zero dynamic subsystem satisfies the following inequality:*

$$\eta^T(t)\Xi(0, \eta(t)) \leq -\lambda_0 \eta^T(t)\eta(t) + \lambda_m(t), \tag{10}$$

where λ_0 is a positive constant and $\lambda_m(t)$ is a bounded function [29].

Remark 2. *Based on Assumption 1, we can establish the following inequality*

$$\|\eta(t)\| \leq \mathcal{K}_1 \|\xi(t)\| + \mathcal{K}_2, \tag{11}$$

where $\mathcal{K}_1, \mathcal{K}_2 > 0$ are the proper constants. What inequality (11) means is that the state vector $\eta(t)$ in (9) is bounded, with the bounded input vector $\xi(t)$. Such a conclusion is called bounded-input bounded-state (BIBS) stability [30], which indicates that the response of the system remains within a certain range in the presence of disturbances or external inputs.

4. Adaptive Inverse Control Scheme For Relative-Degree-One Case with Preisach Hysteresis

This section proposes a control scheme for the relative-degree-one case of the uncertain noncanonical nonlinear neural-network system (6) with input Preisach hysteresis, for which the necessary condition is given in (7), and the procedure for designing the control scheme is detailed as follows.

Preprints (www.preprints.org) | NOT PEER-REVIEWED | Posted: 27 July 2023 doi:10.20944/preprints202307.1915.v1

4.1. System Parameterization

According to Lemma 1, the relative degree of the approximation system (6) is one when it satisfies $CB \neq 0$, which leads to the formulation of the tracking control dynamics subsystem that can be expressed as follows

$$\begin{aligned} \dot{y}(t) &= CAx(t) + CW^{*}S(x(t)) + CBu(t), \\ u(t) &= \mathcal{H}(v(t), \tau_0(\beta, \alpha)), \end{aligned} \tag{12}$$

where the system parameters A, B, C, W^{*} are all unknown. For the tracking control study, the following basic Assumption is needed.

Assumption 2. *Assuming that the sign of the control gain CB in (12) is known and positive [31].*

This assumption guarantees the design procedure of the control scheme is free from any unknown control direction problems.

For ease of adaptive control scheme design, the system (12) needs to be reparameterized. We introduce some new parameters to transform the system into a more suitable form for adaptive control scheme design. Let $\vartheta_1^{*} = [CA, CW^{*}]^T$ represent a parameter vector, $\varpi_1(t) = [x(t), S^T(x(t))]^T$ denote the state vector, and $\mu^{*}(\beta, \alpha) = CB\mu(\beta, \alpha)$ represent the modified density function, and then the system (12) can be expressed as follows

$$\begin{aligned} \dot{y}(t) &= \vartheta_1^{*T}\varpi_1(t) + \mathcal{H}^{*}(v(t), \tau_0(\beta, \alpha)), \\ \mathcal{H}^{*}(v(t), \tau_0) &= \iint_{T_0} \mu^{*}(\beta, \alpha)\gamma_{\alpha\beta}^{*}(v(t), \tau_0)\, d\beta d\alpha. \end{aligned} \tag{13}$$

Assumption 3. *The modified density function $\mu^{*}(\beta, \alpha)$ defined on a finite right triangle plane T_0 takes values between two known nonnegative bounded values $\mu_a(\beta, \alpha)$ and $\mu_b(\beta, \alpha)$ for $\forall(\beta, \alpha) \in T_0$, which means that $\mu_a(\beta, \alpha) \leq \mu^{*}(\beta, \alpha) \leq \mu_b(\beta, \alpha)$.*

Assumption 3 will be used later on in a projection design to equip the adaptive estimate $\hat{\mu}(\beta, \alpha, t)$ of $\mu^{*}(\beta, \alpha)$ with nonnegativity and boundedness properties.

4.2. Implicit Controller Equation

To compensate for the input hysteresis nonlinearity $\mathcal{H}(v(t), \tau_0)$ and to construct a tracking error system with asymptotic convergence property, we develop an adaptive Preisach inverse implicit controller as follows

$$\begin{aligned} &\iint_{T_0} \hat{\mu}(\beta, \alpha, t)\gamma_{\alpha\beta}^{*}(v(t), \tau_0)\, d\beta d\alpha \\ &\quad = -\iota(y(t) - y_m(t)) - \vartheta_1^{T}(t)\varpi_1(t) + \dot{y}_m(t), \end{aligned} \tag{14}$$

where $\hat{\mu}(\beta, \alpha, \cdot)$ and $\vartheta_1(\cdot)$ are the estimates of $\mu^{*}(\beta, \alpha)$ and ϑ_1^{*} respectively, and ι is a positive constant. The implicit controller equation (14) consists of an adaptive Preisach operator with $\hat{\mu}(\beta, \alpha, t)$ as the adaptive estimate of $\mu^{*}(\beta, \alpha)$ on the left sides and the desired output of the adaptive Preisach operator on the right sides. Then, we define

$$\hat{\mathcal{H}}(v(t), \tau_0) = \iint_{T_0} \hat{\mu}(\beta, \alpha, t)\gamma_{\alpha\beta}^{*}(v(t), \tau_0)\, d\beta d\alpha, \tag{15}$$

$$u_d(t) = -\iota(y(t) - y_m(t)) - \vartheta_1^{T}(t)\varpi_1(t) + \dot{y}_m(t), \tag{16}$$

and the implicit controller equation (14) is rewritten as

$$\hat{\mathcal{H}}(v(t), \tau_0) = u_d(t). \tag{17}$$

Preprints (www.preprints.org) | NOT PEER-REVIEWED | Posted: 27 July 2023 doi:10.20944/preprints202307.1915.v1

The next task is to solve the implicit controller equation (17), so that we can computed the control input $v(t)$ in real time. This is essentially equivalent to constructing the inverse function $v(t) = \hat{\mathcal{H}}^{-1}(u_d(t), \tau_0)$, and we will next propose an inverse iterative algorithm to solve it.

A closest match algorithm for solving the implicit controller equation (17) and its convergence proof: Given that the desired output of the adaptive Preisach operator $u_d(t)$ has a continuous, piecewise monotone behavior over the defined time interval $[0, t_E]$, where the partition is

$$0 = t_0 < t_1 < \cdots < t_{N-1} < t_N = t_E, \tag{18}$$

for a positive integer $N \geq 1$, and during each sub-interval $(t_i, t_{i+1}]$, $i = 0, 1, 2, \cdots, N-1$, $u_d(t)$ is monotone. Then, the implicit controller equation (17) will be solved on each sub-interval $(t_i, t_{i+1}]$. It will be shown on the analysis of Remark 4 that the adaptive estimate density function $\hat{\mu}(\beta, \alpha, t)$ changes slowly with time. In this sense, we can assume that $\hat{\mu}(\beta, \alpha, t) = \hat{\mu}(\beta, \alpha, t_i)$ during each sub-intervals $(t_i, t_{i+1}]$, $i = 0, 1, 2, \cdots, N-1$. With this in mind, the adaptive Preisach operator $\hat{\mathcal{H}}(v(t), \tau_0)$ can be expressed as

$$\begin{aligned} \hat{\mathcal{H}}(v(t), \tau_0) = \iint_{T_0} \hat{\mu}(\beta, \alpha, t_i) \gamma^*_{\alpha\beta}(v(t), \tau_0)\, d\beta d\alpha, \\ t \in (t_i, t_{i+1}],\ i = 0, 1, 2, \cdots, N-1. \end{aligned} \tag{19}$$

With a projection design latter, $\hat{\mu}(\beta, \alpha, t)$ is ensured boundedness as $\mu_a(\beta, \alpha) \leq \hat{\mu}(\beta, \alpha, t) \leq \mu_b(\beta, \alpha)$ and nonnegativity for $\forall t > 0$ and $\forall (\beta, \alpha) \in T_0$. Then, from the third equality of (4), it is not hard to prove that the adaptive Preisach operator $\hat{\mathcal{H}}(v(t), \tau_0)$ has monotonicity on each sub-interval $(t_i, t_{i+1}]$, and the output range of $\hat{\mathcal{H}}(v(t), \tau_0)$ can be obtained from the following equation during $(t_i, t_{i+1}]$:

$$H_{i,min} = -\iint_{T_0} \hat{\mu}(\cdot) d\beta d\alpha,\ H_{i,max} = \iint_{T_0} \hat{\mu}(\cdot) d\beta d\alpha.$$

For the implicit controller equation (17) to have a solution, the following constructed saturation condition is necessary:

$$H_{i,min} \leq u_d(t) \leq H_{i,max} \quad \text{for} \quad \forall t \in (t_i, t_{i+1}], \tag{20}$$

where $i = 0, 1, 2, \cdots, N-1$. The limitation of the output range (20) stems from the fact that the Preisach operator $\mathcal{H}(v(t), \tau_0)$ is a saturated hysteresis model and the saturation occurs when the control input $v(t)$ above the upper threshold α_0 or below the lower threshold β_0.

Suppose that the condition (20) is satisfied. There are two discretization steps involved, the discretization of the time interval $[0, t_E]$ has been described in (18) and the discretization range $R = [v_{\min}, v_{\max}]$ of the adaptive Preisach operator (15) input $v(t)$ is uniformly divided into L segments as $V_L = \{\bar{v}_j, j = 1, 2, \cdots, L+1\}$ where $\bar{v}_j = v_{\min} + (j-1)\Delta_v$, $\Delta_v = (v_{\max} - v_{\min})/L$, and L is called the discretization level. The result of discretizing the input range R is that the Preisach plane T_0 is divided into cells. Considering the plane T_0 with discretization degree L, and within each discretization cell, assuming the density function $\hat{\mu}(\beta, \alpha, t)$ on (15) be nonnegative and remains constant. The inversion problem is, given the desired instaneous value of $u_d(t)$, and the memory curve $\Phi(\beta, v(t_d))$ generated by the previous input, to find the corresponding input signal $v^*(t)$ such that the equality $u_d(t) = \hat{\mathcal{H}}(v^*(t), \tau_0)$ is satisfied, which can be calculated by the following algorithm [22]:

Preprints (www.preprints.org) | NOT PEER-REVIEWED | Posted: 27 July 2023 doi:10.20944/preprints202307.1915.v1

[H] **Algorithm 1** Closest Match Algorithm For Adaptive Preisach Operator.

Input: The memory curve $\Phi(\beta, v(t_d))$ and the desired value of $u_d(t)$
Output: Control input $v_L^*(t)$
Step 1) Set $m = 0$, $v^{(m)} = v_{\min}$
Step 2)
if $v^{(m)} = \bar{v}_{L+1}$ **then**
go to Step 5.
else
$v^{(m+1)} = v^{(m)} + \Delta_v$;
$\tilde{\Phi} = \Phi(\beta, v^{(m)})$ (backup the memory curve);
$m = m + 1$;
go to Step 3.
end if
Step 3) Calculate $u_d^{(m)} = \hat{\mathcal{H}}(v^{(m)}, \tau_0)$, and update the memory curve to $\Phi(\beta, v^{(m)})$.
if $u_d^{(m)} = u_d(t)$ **then**
go to Step 5.
else if $u_d^{(m)} < u_d(t)$ **then**
go to Step 2.
else
go to Step 4.
end if
Step 4)
if $|u_d^{(m)} - u_d(t)| \leq |u_d^{(m-1)} - u_d(t)|$ **then**
go to Step 5.
else
$v_L^*(t) = v^{(m-1)}$;
$\Phi(\beta, v_L^*(t)) = \tilde{\Phi}$;
Exit.
end if
Step 5)
$v_L^*(t) = v^{(m)}$;
$\Phi(\beta, v_L^*(t)) = \Phi(\beta, v^{(m)})$;
Exit.

The algorithm is based on the piecewise monotonicity property of the adaptive Preisach operator $\hat{\mathcal{H}}(v(t), \tau_0)$, and it is not hard to see that the algorithm obtains the solution $v_L^*(t)$ in at most L times. The convergence of the above iterative algorithm is given below.

Proposition 1. *Under Assumption 1-3, suppose that condition (20) is satisfied. Then, the iterative algorithm can find a solution $v_L^*(t) = \bar{v}_j \in V_L$ such that*

$$|\hat{\mathcal{H}}(v_L^*(t), \tau_0) - u_d(t)| = \min_{\bar{v}_j \in V_L} |\hat{\mathcal{H}}(\bar{v}_j, \tau_0) - u_d(t)|. \tag{21}$$

Besides, as the discretization degree goes to infinity, we can find the exact solution of the inverse problem, i.e., $\lim_{L\to\infty} v_L^*(t) = v^*(t)$.

Proof. Our task is to prove the piecewise monotonicity and Lipschitz continuity of the adaptive Preisach operator (15), based on this property we can follow the arguments as Proposition 5.1 in [22] to prove Proposition 1.

As previously demonstrated, it has been established that the adaptive Preisach operator (15) can be represented in the form of (19) during the sub-intervals $(t_i, t_{i+1}]$ with the adaptive density function $\hat{\mu}(\beta, \alpha, t_i)$ is nonnegative. Then, from the third equality of (4), the following inequality holds

$$\left(\hat{\mathcal{H}}(v(t_2), \tau_0) - \hat{\mathcal{H}}(v(t_1), \tau_0)\right)\left(v(t_2) - v(t_1)\right) \geq 0, \tag{22}$$

for $\forall t_1, t_2 \in (t_i, t_{i+1}]$. Hence, the adaptive Preisach operator (15) is piecewise monotone on $[0, t_E]$ for the continuous, piecewise monotone control input signal $v(t)$ on $(0, t_E]$. Besides, with the projection design later, the adaptive density function $\hat{\mu}(\beta, \alpha, t_i)$ is guaranteed to be nonnegative and bounded for $\forall t_i \geq 0$, and $\forall(\beta, \alpha) \in T_0$. Then, based on the piecewise expression (19), we can obtain the following Lipschitz continuity property:

$$\left\|\hat{\mathcal{H}}(v(\mathcal{T}_2), \tau_0) - \hat{\mathcal{H}}(v(\mathcal{T}_1), \tau_0)\right\| \leq K_L \left\|v(\mathcal{T}_2) - v(\mathcal{T}_1)\right\|, \tag{23}$$

Preprints (www.preprints.org) | NOT PEER-REVIEWED | Posted: 27 July 2023 doi:10.20944/preprints202307.1915.v1

for $\forall \mathcal{T}_1, \mathcal{T}_2 \in [0, t_E]$, where K_L is a Lipschitz constant.

Based on the piecewise monotonicity (22) and Lipschitz continuity (23) of the adaptive Preisach operator (15), we can follow the arguments as Proposition 5.1 in [22] to prove Proposition 1. □

Up to now, we have provided an iterative algorithm that the control input signal $v(t)$ in the implicit controller equation (17) can be computed iteratively, and finally, the convergence of this iterative algorithm is proved. Next, we will analyze the performances of the adaptive control scheme.

4.3. Performance Analysis

Since the limitations of computation time and the efficiency of the iterative algorithm, obtaining an exact solution within a finite number of iterations is challenging. Therefore, the implicit control equation (14) can be reformulated as follows

$$\begin{aligned} &\iint_{T_0} \hat{\mu}(\beta, \alpha, t) \gamma^*_{\alpha\beta}(v^*_L(t), \tau_0) d\beta d\alpha + \delta(t) \\ &\quad = -\iota(y(t) - y_m(t)) - \vartheta_1^T(t)\omega_1(t) + \dot{y}_m(t), \end{aligned} \tag{24}$$

where $\delta(t)$ is the bounded iteration error. With the iteration results $v^*_L(t)$ as the control input, substituting (13) into (24), we have the tracking error equation as follows

$$\begin{aligned} \dot{e}(t) = &- \iint_{T_0} \tilde{\mu}(\beta, \alpha, t) \gamma^*_{\alpha\beta}\left(v^*_L(t), \tau_0\right) d\beta d\alpha \\ &- \delta(t) - \iota e(t) - \tilde{\vartheta}_1^T(t)\omega_1(t), \end{aligned} \tag{25}$$

where $e(t) = y(t) - y_m(t)$, and the adaptive parameters error $\tilde{\mu}(\beta, \alpha, \cdot) = \hat{\mu}(\beta, \alpha, \cdot) - \mu^*(\beta, \alpha)$ and $\tilde{\vartheta}_1^T(\cdot) = \vartheta_1(\cdot) - \vartheta_1^*$.

Remark 3. *In practical engineering applications, a proper bounded discretization degree L ensures that $|\delta(t)| \leq \epsilon$, where ϵ is an acceptable minor positive constant in engineering applications. Hence, we consider the iterative error $\delta(t)$ as an external disturbance and use the following tracking error equation (26) for the next analysis in this paper.*

$$\begin{aligned} \dot{e}(t) = &- \iint_{T_0} \tilde{\mu}(\beta, \alpha, t) \gamma^*_{\alpha\beta}\left(v^*_L(t), \tau_0\right) d\beta d\alpha \\ &- \iota e(t) - \tilde{\vartheta}_1^T(t)\omega_1(t). \end{aligned} \tag{26}$$

By considering the tracking error equation (26), we choose the positive definite function as

$$V(e, \tilde{\mu}) = \frac{1}{2\phi} \iint_T \tilde{\mu}^2(\beta, \alpha, \cdot) d\beta d\alpha + \frac{1}{2} e^2 + \frac{1}{2} \tilde{\vartheta}_1^T \Gamma_1^{-1} \tilde{\vartheta}_1, \tag{27}$$

where $\Gamma_1 = \Gamma_1^T > 0$ and $\phi > 0$ are the adaptive parameters for adaptive laws. Then, the time derivation of $V(e, \tilde{\mu})$ is

$$\begin{aligned} \dot{V} = &- \frac{1}{\phi} \iint_T \tilde{\mu}(\beta, \alpha, t) \left(\phi \gamma^*_{\alpha\beta}\left(v^*_L(t), \tau_0\right) e(t) - \frac{\partial}{\partial t} \hat{\mu}(\beta, \alpha, t) \right) d\beta d\alpha \\ &- \iota e^2(t) - \tilde{\vartheta}_1^T \Gamma_1^{-1} (\Gamma_1 \omega_1(t) e(t) - \dot{\vartheta}_1(t)). \end{aligned} \tag{28}$$

Preprints (www.preprints.org) | NOT PEER-REVIEWED | Posted: 27 July 2023 doi:10.20944/preprints202307.1915.v1

Lyapunov-based adaptive control scheme: To make $\dot{V} \leq 0$, the update laws for the estimates $\vartheta(t)$ and $\hat{\mu}(\beta, \alpha, t)$ are chosen as

$$\dot{\vartheta}_1(t) = \Gamma_1 \omega_1(t) e(t), \tag{29}$$

$$\frac{\partial}{\partial t}\hat{\mu}(\beta,\alpha,t) = \begin{cases} \phi\gamma^*(t)e(t) & \text{if } \hat{\mu} \in (\mu_a, \mu_b), \text{ or} \\ & \text{if } \hat{\mu} = \mu_a,\ \gamma^*(t)e(t) \geq 0, \text{ or} \\ & \text{if } \hat{\mu} = \mu_b,\ \gamma^*(t)e(t) \leq 0, \\ 0, & \text{otherwise,} \end{cases} \tag{30}$$

where $\gamma^*(t)$, $\hat{\mu}$, μ_a and μ_b are the brief representations of $\gamma^*_{\alpha\beta}\left(v^*_L(t), \tau_0\right)$, $\hat{\mu}(\beta, \alpha, t)$, $\mu_a(\beta, \alpha)$ and $\mu_b(\beta, \alpha)$, respectively. By choosing the initial value of $\hat{\mu}(\beta, \alpha, t)$ within the range $[\mu_a(\beta, \alpha), \mu_b(\beta, \alpha)]$, the projection design (30) ensures that $\mu_a(\beta, \alpha) \leq \hat{\mu}(\beta, \alpha, t) \leq \mu_b(\beta, \alpha)$ and $\tilde{\mu}(\beta, \alpha, t)\left(\phi\gamma^*_{\alpha\beta}\left(v^*_L(t), \tau_0\right)e(t) - \frac{\partial}{\partial t}\hat{\mu}(\beta, \alpha, t)\right) \geq 0$ for $\forall t \geq 0$. Therefore, we have the following results for the $\lim_{t\to\infty} e(t) = 0$.

Theorem 1. *Under Assumptions 1-3 and Proposition 1, all signals in the closed-loop system consisted of the noncanonical nonlinear system (6), the Preisach operator (2), the iterative inverse algorithm, and the implicit controller (14) which is updated by the adaptive laws (29)-(30), are bounded, and the tracking error $e(t)$ satisfies*

$$\lim_{t\to\infty} e(t) = 0.$$

Proof. Substitute the adaptive laws (29)-(30) into the derivation of V (28), we can derive that

$$\dot{V} \leq -\iota e^2(t). \tag{31}$$

Since ι is a positive constant, we have $\dot{V} \leq 0$. Then, $e(t)$, $\vartheta_1(t)$, and $\hat{\mu}(\beta, \alpha, t)$ are bounded, which implies that $y(t)$ is bounded. From Assumption 1, we can establish the inequality that $\|\eta(t)\| \leq \mathcal{K}\|y(t)\| + \mathcal{K}$ for a proper constant $\mathcal{K}$, thus $\eta(t)$ and $x(t)$ are bounded. From the desired output of the adaptive Preisach operator (16), we can derive the boundedness of $u_d(t)$, then, the boundedness of all the closed-loop signals is established. Next, we will show the properties that $e(t) \in L^2$ and $\lim_{t\to\infty} e(t) = 0$. Integrating both sides of the first inequality in the derivation of V in (31) yields that $\int_0^\infty e^2(t)dt < \infty$, so $e(t) \in L^2$. From the tracking error equation (26), it clearly shows that $\dot{e}(t)$ is bounded. Therefore, using Barbalat's Lemma, we can obtain that $\lim_{t\to\infty} e(t) = 0$. □

Remark 4. *Since $e(t) \in L^2 \cap L^\infty$ and $\lim_{t\to\infty} e(t) = 0$, with the projection design in (30), it is not hard to derive that*

$$\frac{\partial}{\partial t}\hat{\mu}(\beta,\alpha,t) \in L^2 \cap L^\infty, \text{ and } \lim_{t\to\infty}\frac{\partial}{\partial t}\hat{\mu}(\beta,\alpha,t) = 0, \tag{32}$$

which means that $\hat{\mu}(\beta, \alpha, t)$, the adaptive estimate of $\mu^*(\beta, \alpha)$, changes very slowly and eventually converges to a time-independent value $\hat{\mu}^*(\beta, \alpha)$. Besides, the adaptive estimate $\hat{\mu}(\beta, \alpha, t)$ is limited to a compact set $[\mu_a(\beta, \alpha), \mu_b(\beta, \alpha)]$ by the projection design (30), which means that the $\hat{\mu}(\beta, \alpha, t)$ would not be large. Then, during on each sub-interval $(t_i, t_{i+1}]$, $i = 0, 1, 2, \cdots, N-1$, we can consider $\hat{\mu}(\beta, \alpha, t) = \hat{\mu}(\beta, \alpha, t_i)$ on the iterative algorithm for $\forall t \in (t_i, t_{i+1}]$, and would not affect the performance of the system.

5. Simulation Study

This section presents the simulation results for the relative-degree-one case of noncanonical nonlinear approximation system (6) with unknown parameters and preceded by the Preisach hysteresis operator. The purpose in this section is to provide strong evidence for the proposed adaptive control

Preprints (www.preprints.org) | NOT PEER-REVIEWED | Posted: 27 July 2023 doi:10.20944/preprints202307.1915.v1

scheme in achieving the desired tracking performance as illustrated in Theorem 1, which guarantees the tracking error converges to zero as time goes to infinity.

5.1. Experimental Equipment

We developed a piezoactuator-driven stage as the experimental platform, which mainly consists of four parts: 1) an E01 piezoelectric ceramic controller including a communication module E18.i3, a sensor control module E09.S3/L3 and a power amplifier module E03.00, which has a voltage output range of 0-150 V; 2) a piezoelectric actuator, which has a displacement output of 0-40 μm; 3) a vibration isolation table, which serves the purpose of isolating the experiment equipment from external vibration; 4) a computer with MATLAB R2020a (see Figure 3).

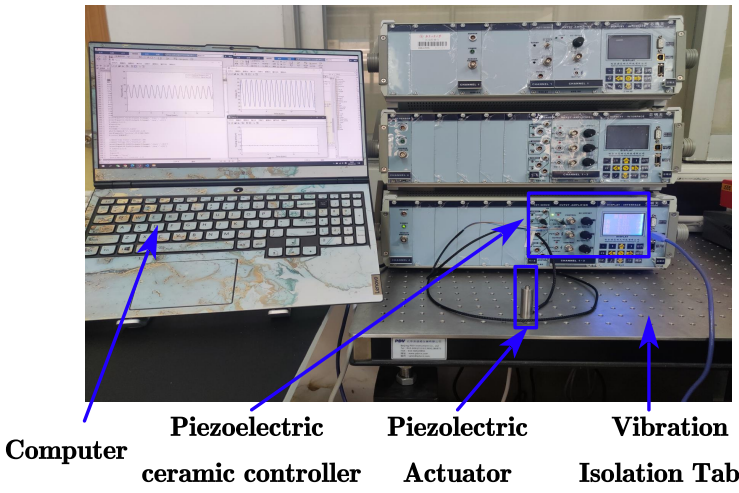

Figure 3. Experimental platform

5.2. Hysteresis Identification

As the only parameter of the Preisach operator, the upper and lower bounds of the density function $\mu(\beta, \alpha)$ play an important role in ensuring the convergence of the iterative algorithm. Unreasonable settings of these bounds can seriously affect output accuracy. Therefore, it is necessary to perform systematic identification of the actual piezoelectric actuator, and then determine the upper and lower bounds of the estimator $\hat{\mu}(\beta, \alpha, t)$ based on the identification result. With this in mind, we employ a gradient descent algorithm to identify the density function. In this experiment, a triangular wave is chosen as the voltage input signal $v(t)$ at 5 Hz with a range from 0 V to 115 V and we set the sampling rate as 1 kHz. Then, the identified density function is shown in Figure 4a. To evaluate the hysteresis curve matching degree between the one generated by the Preisach operator with identified density function and the experiment measurement, the voltage input is chosen as a triangular wave signal at 5 Hz within the range of -55V to 55V and the result is shown in Figure 4b, which provides a close resemblance between the two curves.

5.3. Simulation System Modeling

In the simulation experiments, we follow the noncanonical nonlinear approximation system (6) for the system parameter design, where $B = [2, 1]^T, C = [1, -1]$,

$$A = \begin{bmatrix} 2 & 1 \\ 0 & 1 \end{bmatrix}, \quad \mathcal{W}^* = \begin{bmatrix} 2.0 & -0.6 \\ 1.2 & 0.2 \end{bmatrix}, \tag{33}$$

Preprints (www.preprints.org) | NOT PEER-REVIEWED | Posted: 27 July 2023 doi:10.20944/preprints202307.1915.v1

and the activation functions vector $S(x) = [S_1(x), S_2(x)]^T$ with

$$S_1(x) = \frac{3}{1+e^{-2x_2}} - 1.5, \quad S_2(x) = \left(\frac{4}{1+e^{-2x_2}} - 2\right)\left(\frac{3}{1+e^{-2x_1}} - 1.5\right). \tag{34}$$

The Preisach operator plane is defined by the thresholds $\beta_0 = -59$ and $\alpha_0 = 59$.

The initial control input is chosen as $v(0) = 0$, with the definition of memory curve, we have $\Phi(\beta, 0) = 0$. The initial output of Preisach operator is $\mathcal{H}(v(0), \tau_0(\beta, \alpha)) = 0.558$ with the density function $\mu(\beta, \alpha)$ obtained from identification. The initial value of the state vector is chosen as $x(0) = [0.6, 0]^T$, and a basic sinusoidal function $y_m(t) = 2\sin(t) + 2.5$ is chosen as the reference signal.

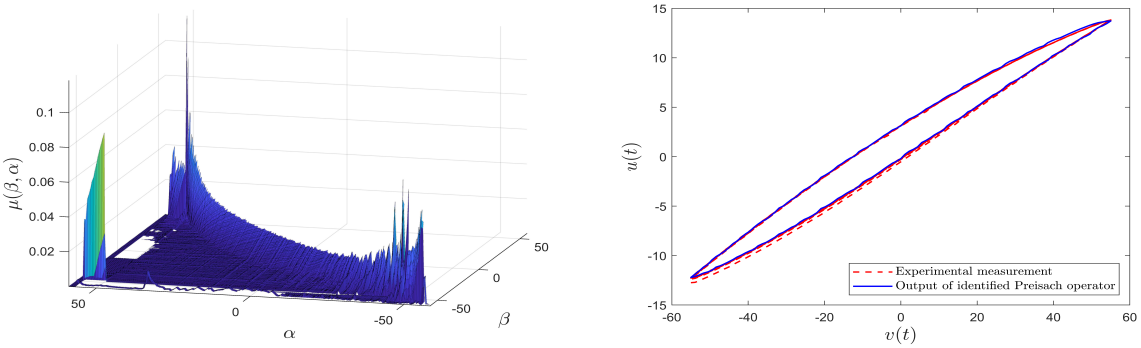

(a) **(b)**

Figure 4. The identification results of piezoelectric actuator. (**a**) The identified density function $\mu(\beta, \alpha)$ of the Preisach operator. (**b**) Matching degree of Preisach operator with identified density function to the experimental measurement of the hysteresis curve.

5.4. Simulation Results

Initial parameters and design parameters: It is not hard to derive that the simulation system satisfies the condition: $CB \neq 0$, and then the adaptive scheme for relative-degree-one case in Section 4 can be used to control this system. With the diffeomorphism $\Omega(x) = [\xi, \eta]^T = [x_1 - x_2, -x_1 + 2x_2]^T$, the noncanonical nonlinear approximation system (6) can be transformed into a tracking dynamics subsystem and a zero dynamics subsystem with BIBS stability, and satisfies the Assumption 1. By a simple calculation, the norminal parameters are $\vartheta_1^* = [2, 0, 0, 0.8]^T$, $\mu^*(\beta, \alpha) = CB\mu(\beta, \alpha)$, which are unknown for the control design and estimated by $\vartheta_1(t)$ and $\hat{\mu}(\beta, \alpha, t)$, respectively. The lower and upper bounds of $\mu^*(\beta, \alpha)$ are chosen as $\mu_a(\beta, \alpha) = 0$ and $\mu_b(\beta, \alpha) = 1.1\mu(\beta, \alpha)$ for the projection design, where $\mu(\beta, \alpha)$ is obtained from the identification result. The initial parameters are chosen as $\vartheta_1(0) = 0.5\vartheta_1^*$ and $\hat{\mu}(\beta, \alpha, 0) = 0.7\mu(\beta, \alpha)$. Other design parameters are chosen as $\iota = 4$, $\phi = 0.08$ and $\Gamma_1 = \text{diag}\{1, 0.8, 0.8, 1.2\}$.

Simulation results and analysis: By employing the proposed adaptive control scheme in the simulation system, the tracking performance is depicted in Figure 5a which confirms the desired behavior of the control scheme and shows that the output $y(t)$ converges to the reference signal $y_m(t)$ over time. Figure 5b shows that the tracking error $e(t)$ gradually diminishes and eventually converges to zero over time. Furthermore, Figure 5c shows the boundedness of the system input $u(t)$ and control input $v(t)$. As an example to confirm that the estimate $\hat{\mu}(\beta, \alpha, t)$ changes very slow and eventually converge to a time-independent value $\hat{\mu}^*(\beta, \alpha)$ as illustrated in Remark 4, Figure 5d shows the trajectories of $\hat{\mu}(30, 50)$ and $\hat{\mu}(-50, -30)$ vs. time. With the discretization level $L = 118$, Figure 6a shows that the iteration error $\hat{\mathcal{H}}(v_L^*(t), \tau_0) - u_d(t)$ is within the range of $\pm 0.2\mu m$, where the control input $v_L^*(t)$ is calculated using the iterative algorithm in the implicit control equation (17). The results confirm the convergence of the iterative algorithm established in Proposition 1. The effectiveness of

Preprints (www.preprints.org) | NOT PEER-REVIEWED | Posted: 27 July 2023 doi:10.20944/preprints202307.1915.v1

iterative algorithm is shown in Figure 6b, we can see that the desired one $u_d(t)$ is well achieved by the adaptive operator $\hat{\mathcal{H}}(v(t), \tau_0)$.

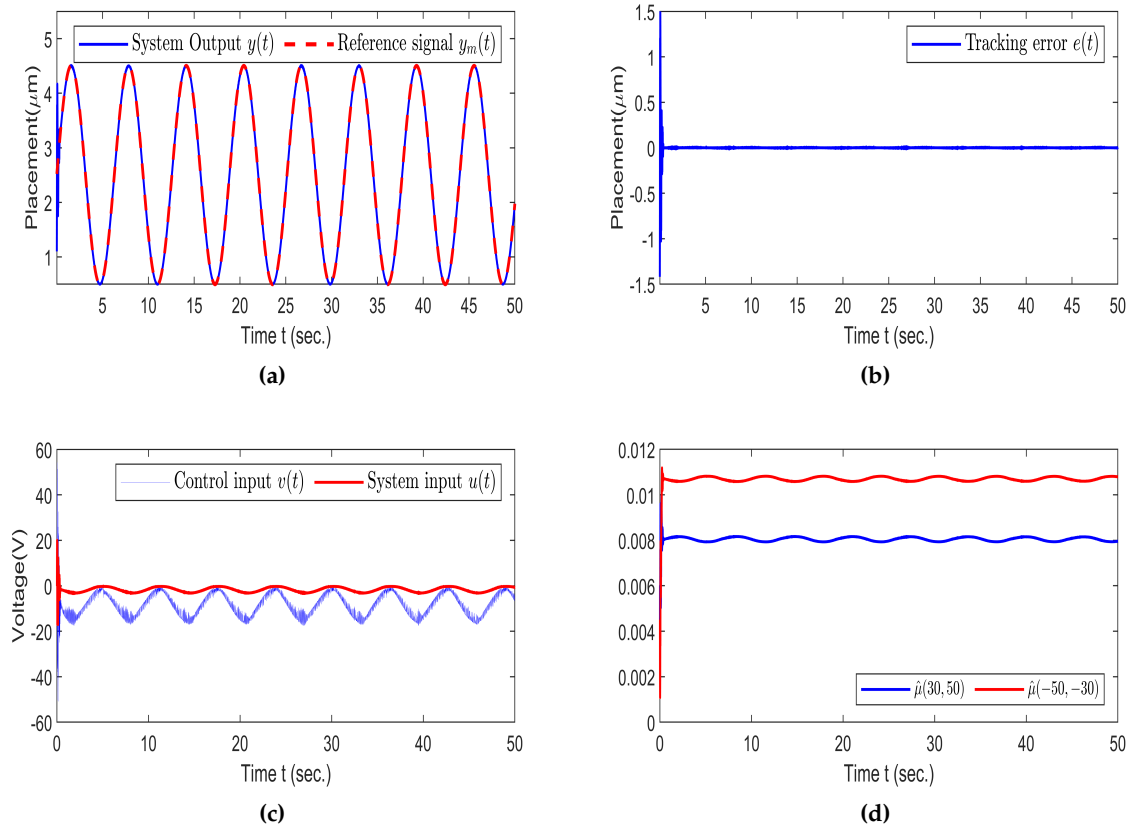

Figure 5. System response with $y_m(t) = 2\sin(t) + 2.5$. (**a**) Tracking performance $y(t)$ and $y_m(t)$ versus time(s). (**b**) Tracking error $e(t)$ versus time(s). (**c**) Control input $v(t)$ and system input $u(t)$ versus time(s). (**d**) Estimators $\hat{\mu}(30, 50)$ and $\hat{\mu}(-50, -30)$ versus time(s).

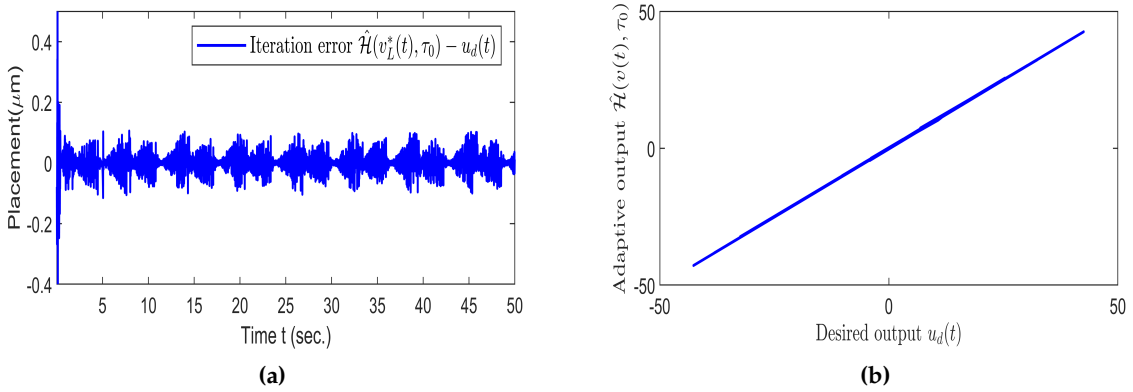

Figure 6. Iterative algorithm performance.

6. Conclusion

We have developed an iterative inverse-based adaptive control scheme for the uncertain nonlinear system in the noncanonical form with unknown input Preisach hysteresis. The control scheme utilizes a new adaptive version of the closest match algorithm to effectively compensate for the unknown hysteresis effects. The convergence of the iterative algorithm was established by demonstrating the piecewise monotonicity and Lipschitz continuity of the adaptive Preisach operator $\hat{\mathcal{H}}(v(t), \tau_0)$.

Furthermore, we conducted the complete stability analysis of the closed-loop system. The simulation results serve as strong evidence for the proposed control scheme in achieving desired tracking performance.

Author Contributions: Conceptualization, G.L.; methodology, W.Y.; software, G.D.; validation, G.L. and G.D.; formal analysis, G.D. and X.W.; writing—original draft preparation, W.Y.; writing—review and editing, W.L.and X.W., G.D. and X.S; All authors have read and agreed to the published version of the manuscript.

Funding: This research was funded by the Tertiary Education Scientific research project of Guangzhou Municipal Education Bureau [No.202235364], and the Special projects in key fields of colleges and universities in Guangdong Province [No.2021ZDZX1109], and the Research project of Guangzhou City Polytechnic[No.KYTD2023004], and the National Natural Science Foundation of China [No.6210021076], and the Guangzhou Municipal Science and Technology Project [No.202201010381].

Institutional Review Board Statement: Not applicable.

Informed Consent Statement: Not applicable.

Data Availability Statement: Not applicable.

Acknowledgments: Not applicable.

Conflicts of Interest: The authors declare no conflict of interest.

Reference

1. Zaman, S.; Leyva, A.; Hassan, M.S.; Valladolid, A.; Herrera, N.E.; Gomez, S.G.; Mahmud, M.S.; Tucker, D.; Haynes, C.; Lin, Y. Implementation of Smart Materials for Actuation of Traditional Valve Technology for Hybrid Energy Systems. *Actuators* **2023**, *12*.
2. Frolova, L.; Ryba, T.; Diko, P.; Kavecansky, V.; Milkovic, O.; Dzubinska, A.; Reiffers, M.; Vargova, Z.; Varga, R. Smart Shape Memory Actuator Based on Monocrystalline Ni2FeGa Glass-Coated Microwire. *IEEE Transactions on Magnetics* **2018**, *54*, 1–5.
3. Bocchetta, G.; Fiori, G.; Sciuto, S.A.; Scorza, A. Performance of Smart Materials-Based Instrumentation for Force Measurements in Biomedical Applications: A Methodological Review. *Actuators* **2023**, *12*.
4. Chen, L.; Niu, Y.; Yang, X.; Zhu, W.L.; Zhu, L.M.; Zhu, Z. A Novel Compliant Nanopositioning Stage Driven by a Normal-Stressed Electromagnetic Actuator. *IEEE Transactions on Automation Science and Engineering* **2022**, *19*, 3039–3048.
5. Baziyad, A.G.; Ahmad, I.; Salamah, Y.B.; Alkuhayli, A. Robust Tracking Control of Piezo-Actuated Nanopositioning Stage Using Improved Inverse LSSVM Hysteresis Model and RST Controller. *Actuators* **2022**, *11*.
6. Chen, L.; Zhu, Y.; Ling, J.; Zhang, M. Development and Characteristic Investigation of a Multidimensional Discrete Magnetostrictive Actuator. *IEEE/ASME Transactions on Mechatronics* **2022**, *27*, 2071–2079.
7. Adly, A.; Mayergoyz, I.; Bergqvist, A. Preisach modeling of magnetostrictive hysteresis. *Journal of Applied Physics* **1991**, *69*, 5777–5779.
8. Preisach, F. Über die magnetische Nachwirkung. *Zeitschrift für physik* **1935**, *94*, 277–302.
9. Li, R.; Feng, Y.; Hu, Z. Dynamic Surface Control of Shape Memory Alloy Actuating Systems with Inverse Duhem Hysteresis Compensation. 2018 IEEE International Conference on Mechatronics and Automation (ICMA). IEEE, 2018, pp. 1305–1310.
10. Brokate, M.; Sprekels, J. Hysteresis and Phase Transitions. *Springer New York eBooks* **1996**.
11. Rehman, O.U.; Petersen, I.R. Using inverse nonlinearities in robust output feedback guaranteed cost control of nonlinear systems. *IEEE Transactions on Automatic Control* **2014**, *60*, 1139–1144.
12. Köhler, J.; Soloperto, R.; Müller, M.A.; Allgöwer, F. A computationally efficient robust model predictive control framework for uncertain nonlinear systems. *IEEE Transactions on Automatic Control* **2020**, *66*, 794–801.
13. Wang, A.; Liu, L.; Qiu, J.; Feng, G. Event-triggered robust adaptive fuzzy control for a class of nonlinear systems. *IEEE Transactions on Fuzzy Systems* **2018**, *27*, 1648–1658.
14. Li, Z.; Shan, J.; Gabbert, U. Inverse compensation of hysteresis using Krasnoselskii-Pokrovskii model. *IEEE/ASME Transactions on Mechatronics* **2018**, *23*, 966–971.

15. Li, Z.; Shan, J.; Gabbert, U. A direct inverse model for hysteresis compensation. *IEEE Transactions on Industrial Electronics* **2020**, *68*, 4173–4181.
16. Li, Z.; Su, C.Y.; Chai, T. Compensation of hysteresis nonlinearity in magnetostrictive actuators with inverse multiplicative structure for Preisach model. *IEEE Transactions on Automation Science and engineering* **2013**, *11*, 613–619.
17. Zhang, J.; Iyer, K.; Simeonov, A.; Yip, M.C. Modeling and inverse compensation of hysteresis in supercoiled polymer artificial muscles. *IEEE Robotics and Automation Letters* **2017**, *2*, 773–780.
18. Li, Z.; Shan, J.; Gabbert, U. Inverse compensator for a simplified discrete Preisach model using model-order reduction approach. *IEEE Transactions on Industrial Electronics* **2018**, *66*, 6170–6178.
19. Visone, C. Hysteresis modelling and compensation for smart sensors and actuators. Journal of Physics: Conference Series. IOP Publishing, 2008, Vol. 138 1, p. 012028.
20. Tan, X.; Venkataraman, R.; Krishnaprasad, P.S. Control of hysteresis: Theory and experimental results. Smart Structures and Materials 2001: Modeling, Signal Processing, and Control in Smart Structures. SPIE, 2001, Vol. 4326, pp. 101–112.
21. Iyer, R.V.; Tan, X. Control of hysteretic systems through inverse compensation. *IEEE Control Systems Magazine* **2009**, *29*, 83–99.
22. Iyer, R.V.; Tan, X.; Krishnaprasad, P. Approximate inversion of the Preisach hysteresis operator with application to control of smart actuators. *IEEE Transactions on automatic control* **2005**, *50*, 798–810.
23. Tan, X.; Baras, J.S. Adaptive identification and control of hysteresis in smart materials. *IEEE Transactions on automatic control* **2005**, *50*, 827–839.
24. Tan, X.; Baras, J.S. Modeling and control of hysteresis in magnetostrictive actuators. *Automatica* **2004**, *40*, 1469–1480.
25. Li, Z.; Zhang, X.; Su, C.Y.; Chai, T. Nonlinear Control of Systems Preceded by Preisach Hysteresis Description: A Prescribed Adaptive Control Approach. *IEEE Transactions on Control Systems Technology* **2016**, *24*, 451–460.
26. Zhang.; Yanjun.; Tao.; Gang.; Chen.; Mou.. Adaptive Neural Network Based Control of Noncanonical Nonlinear Systems. *IEEE Transactions on Neural Networks & Learning Systems* **2016**.
27. Isidori, A. *Nonlinear Control Systems*; Springer Science & Business Media, 1995.
28. Ma, X.; Tao, G. Adaptive actuator compensation control with feedback linearization. *IEEE Transactions on Automatic Control* **2000**, *45*, 1705–1710.
29. Sastry, S.; Bodson, M.; Bartram, J.F. Adaptive control: stability, convergence, and robustness, 1990.
30. Ioannou, P.A.; Sun, J. *Robust adaptive control*; Vol. 1, PTR Prentice-Hall Upper Saddle River, NJ, 1996.
31. Lai, G.; Tao, G.; Zhang, Y.; Liu, Z. Adaptive control of noncanonical neural-network nonlinear systems with unknown input dead-zone characteristics. *IEEE Transactions on Neural Networks and Learning Systems* **2019**, *31*, 3346–3360.